


Distinct Airway Microbiome and Metabolite Profiles in Eosinophilic and Neutrophilic Asthma

Shuang Liu^{1,*}, Zhiwei Lin^{1,2,*}, Jiayong Zhou^{3,*}, Xiaojing Yang², Liuyong You¹, Qian Yue Yang¹, Tianyang Li¹, Zhaoming Hu¹, Xuyan Zhan¹, Yueting Jiang¹, Baoqing Sun¹ 

¹Department of Clinical Laboratory, Guangzhou Institute of Respiratory Health, State Key Laboratory of Respiratory Disease, National Center for Respiratory Medicine, National Clinical Research Center for Respiratory Disease, Guangzhou Laboratory, The First Affiliated Hospital of Guangzhou Medical University, Guangzhou, People's Republic of China; ²Respiratory Mechanics Laboratory, State Key Laboratory of Respiratory Disease, National Center for Respiratory Medicine, National Clinical Research Center for Respiratory Disease, Guangzhou Institute of Respiratory Health, Guangzhou, 510120, People's Republic of China; ³Guangzhou Center for Disease Control and Prevention (Guangzhou Health Supervision Institute), Guangzhou, 510440, People's Republic of China

*These authors contributed equally to this work

Correspondence: Baoqing Sun; Yueting Jiang, Department of Clinical Laboratory, Guangzhou Institute of Respiratory Health, State Key Laboratory of Respiratory Disease, National Center for Respiratory Medicine, National Clinical Research Center for Respiratory Disease, Guangzhou Laboratory, The First Affiliated Hospital of Guangzhou Medical University, Guangzhou, People's Republic of China, Email sunbaoqing@vip.163.com; jyting8899@126.com

Background: Asthma is a chronic, heterogeneous disease driven by inflammatory phenotypes, primarily eosinophilic asthma (EA) and neutrophilic asthma (NEA). While allergen triggers are well-known, the role of the airway microbiome and metabolites in asthma exacerbations remains poorly understood.

Methods: We recruited 64 participants (24 EA, 20 NEA, 20 healthy controls [HC]) for the discovery cohort, with validation in an external cohort (10 EA, 8 NEA, 8 HC). Induced sputum samples were analyzed using 16S rRNA sequencing to profile bacterial composition and non-targeted metabolomics to assess airway metabolites. Random forest models identified diagnostic markers, validated in the external cohort.

Results: Significant shifts in airway microbiota were observed, particularly between NEA and HC, and between EA and NEA. Four bacterial general-*Stenotrophomonas*, *Streptococcus*, *Achromobacter*, and *Neisseria*-were consistently identified across groups. *Veillonella* was more abundant in NEA vs HC, while *Achromobacter* was enriched in NEA vs EA, indicating distinct microbial signatures. Metabolomic profiling revealed distinct pathways: pyrimidine metabolism (EA vs HC), tryptophan metabolism (NEA vs HC), and arachidonic acid metabolism (EA vs NEA). Microbial-metabolite correlations indicated microbiota-driven metabolic activity. Biomarker candidates were validated in the external cohort.

Conclusion: The airway microbiota and metabolites are intricately linked to asthma exacerbations, with distinct patterns between EA and NEA. These findings highlight their potential as diagnostic biomarkers and therapeutic targets for personalized asthma management.

Keywords: eosinophilic, neutrophils asthma, 16S rRNA amplicon sequencing, metabolomics, biomarker

Introduction

Asthma is a chronic and heterogeneous disease characterized by airway inflammation and hyperresponsiveness, manifesting in several inflammatory phenotypes.^{1,2} Among these, eosinophilic asthma (EA) and neutrophilic asthma (NEA) are two prominent phenotypes, each associated with distinct immune responses and clinical features.^{3,4} These phenotypes differ notably in their pathogenesis and response to corticosteroids. While EA typically responds well to corticosteroid therapy, NEA often exhibits steroid resistance and is frequently observed in severe asthma cases, where the use of macrolides may be necessary.^{5,6} Despite these well-characterized clinical distinctions, considerable gaps remain in understanding the underlying microbial and metabolic landscapes of these phenotypes. Furthermore, biomarkers to differentiate EA and NEA remain limited, with clinical assessments largely relying on cell counts in blood and sputum.

Identifying novel biomarkers for these distinct asthma endotypes could provide deeper insights into disease mechanisms and guide personalized treatment strategies.

Environmental triggers such as allergens and cold air are well-established contributors to asthma exacerbations.⁷ However, emerging evidence supports the hygiene hypothesis, which suggests that increased microbial exposure may reduce asthma risk.⁸ The respiratory microbiota plays a critical role in shaping immune responses, and even small shifts in microbial composition can significantly impact host immunity due to variations in bacterial ligands and metabolite production.⁹ The respiratory tract harbors a diverse bacterial community, with substantial shifts in richness and diversity along its length, from the nasal cavity to the lungs.¹⁰ These microbial changes have been implicated in several respiratory diseases, including lung cancer,¹¹ asthma¹² and chronic obstructive pulmonary disease (COPD).⁹ Growing evidence shows microbiota significantly influence asthma development, with distinct microbial patterns observed across disease severity, treatments, and age groups. Severe asthma exhibits reduced microbial diversity with more *Proteobacteria*, while mild cases show altered *Firmicutes/Bacteroidetes* ratios.¹³ Asthma patients exhibit characteristic alterations in their microbiome following corticosteroid treatment. The oral microbiome demonstrated significant reductions in both *Absoconditabacteriales* and *Bifidobacterium*, nasal microbiota exhibits the most significant alterations, particularly down-regulation of *Porphyromonas* and *Prevotella*.¹⁴ Importantly, children with asthma have delayed microbiota development, while elderly patients show *Bacteroides*-dominated profiles.¹⁵ The specific role of microbiota in the pathogenesis of asthma, particularly in relation to distinct inflammatory phenotypes such as EA and NEA, remains poorly understood. Understanding the relationship between airway microbiota and asthma phenotypes could offer new insights into disease mechanisms and help identify prognostic markers for EA and NEA.

Metabolomics, the comprehensive study of small molecules involved in metabolic processes, has become a powerful tool for discovering biomarkers and elucidating disease mechanisms.¹⁶ Recent research has underscored the interplay between lung microbiota metabolites and respiratory health, showing that microbial-derived metabolites can influence disease progression. Yuan et al highlighted the correlation between the respiratory microbiome and serum metabolomics, suggesting microbial influence on metabolic activity.¹⁷ However, research integrating microbiome and metabolomic data in the context of distinct asthma phenotypes remains limited.¹⁸ Integrating microbiome and metabolomics data, particularly within the lung, could reveal novel pathways involved in EA and NEA pathogenesis and enhance the development of diagnostic and therapeutic strategies.

In this study, we used 16S rRNA sequencing for bacterial profiling and non-targeted metabolomics on sputum from EA, NEA patients, and HC. By comparing microbial and metabolite profiles, we aimed to explore distinct microbial-metabolite correlations. This approach sought unique pathways in asthma subtypes, potentially identifying biomarkers and targets. Our findings offer insights for personalized asthma management.

Materials and Methods

Study Population

Patients with diagnosed asthma were recruited from the First Affiliated Hospital of Guangzhou Medical University between April 2023 and June 2024. Asthma diagnosis followed the Global Initiative for Asthma (GINA) guidelines,¹⁹ according to fulfilment of 1 or more of the following criteria: (1) an increase > 12% in forced expiratory volume in 1 second (FEV1) and an increase > 200 mL after inhalation of 400 µg of albuterol; (2) a 20% reduction in FEV1 in response to a provocative concentration of inhaled methacholine (PC20 < 10 mg/mL); (3) and/or an increase > 20% in FEV1 after 2 weeks of treatment with systemic oral corticosteroids (OCS) or inhaled corticosteroids (ICS).²⁰ (4) Participants were aged between 18 and 70 years. (5) All study participants attended a single visit that encompassed assessments of lung function, asthma symptoms, asthma-specific quality of life, and medication use. We enrolled patients and Healthy control (HC) with no history of smoking. (6) Patients were initially diagnosed with mild-to-moderate asthma exacerbation or persistent asthma according to the American Thoracic Society guidelines and GINA guidelines.²¹ (7) Patients had been routinely treated with fluticasone or an equivalent dose of inhaled corticosteroids for over 6 months but had experienced more than 1 acute exacerbations in the past half year. Exclusion criteria: History of chronic lung diseases or any other diagnosed conditions, ongoing

immunotherapy, malignancy diagnosis, current/recent ex-smokers (<1 year), recent respiratory infection, or antibiotic use in past 4 weeks.

Samples Collection

Sputum induction involved isotonic saline with a bronchodilator, processed as in.¹⁴ ICS and LABAs were stopped for 24 hours.²² Asthma patients were classified as EA or NEA based on sputum cell counts.²³ EA had $\geq 3\%$ eosinophils; NEA had $< 3\%$ eosinophils and neutrophil thresholds of $\geq 75.57\%$ (<20 years), $\geq 61.61\%$ (20–40 years), $\geq 63.25\%$ (40–60 years), or $\geq 67.25\%$ (>60 years). Samples with $> 10\%$ squamous cells were excluded. Precipitates were used for microbiome analysis, supernatants stored at -80°C for metabolism analysis.²⁴ All participants underwent spirometry per ERS guidelines to assess lung function and airway obstruction severity. Included patients had mild-to-moderate, clinically stable exacerbations safe for bronchoscopy.

Ethical approval was obtained from the Ethics Committee of The First Affiliated Hospital of Guangzhou Medical University, with approval codes 2022 No.121 and 2024 No. G-007. Written informed consent was obtained from all participants prior to inclusion in the study. This study was conducted in accordance with the ethical principles of the Declaration of Helsinki. A schematic representation of the study can be found in [Figure 1](#).

16S rRNA Amplicon Sequencing

Microbial DNA from sputum was extracted using the FastDNA Spin Kit and purity was checked with a Nanodrop. Integrity was assessed via agarose gel electrophoresis. PCR amplified the V3-V4 regions of the 16S rRNA gene according to universal primers (515F: 5'-GGACTACHVGGGTWTCTAAT-3', 806R: 5'-GGACTACHVGGGTWTCTAAT-3'). PCR products were purified, quantified, and sequenced on an Illumina NovaSeq6000 at the Novogene Bioinformatics Technology Co., Ltd. The paired-end reads were assigned using barcode and then were merged with FLASH (Fast Length Adjustment of SHort reads) (V1.2.11) software.²⁵ High-quality filtering of the raw tags was performed to obtain clean tags using QIIME (Quantitative Insights into Microbial Ecology) (Version QIIME2-202202). After that, chimeric sequences were compared with Silva Database and using the UCHIME algorithm to detect and remove chimera sequences. A final effective sequence analysis was performed using Uparse software (Uparse V7.0.1001).²⁶

Microbiomics Study

Sequences with a similarity index greater than 97% were assigned to the same operational taxonomic units (OTUs). Alpha diversity metrics (Chao1, Shannon Diversity, Simpson, and Richness indice) were calculated for the OTU table using alpha rarefaction. The beta diversity metric was calculated on the OTU table and visualized using principal coordinate analysis (PCoA) and non-metric multidimensional scaling (NMDS) analysis. The alpha diversity and beta diversity analysis were calculated with QIIME software (version 1.9.1) and displayed with R software (version 2.15.3). Metagenomeseq test was used to calculate significant differences between two groups. Metabolic function was predicated with Phylogenetic Investigation of Communities by Reconstruction of Unobserved States (PICRUSt) based on the high-quality tags of the microbiota.²⁷ Random forest analysis was the classification of samples based on a machine learning model for the purpose of filtering variables.

Non-Targeted Metabolomics Profiling

Metabolites were extracted from sputum and tested with a liquid chromatography-tandem mass spectrometry (LC-MS/MS). The metabolomics analysis was performed using a Vanquish UHPLC system (ThermoFisher, Germany) in Novogene Co., Ltd. (Beijing, China). Samples were injected onto a Hypersil Gold column (100×2.1 mm, 1.9 μm) using a 12-min linear gradient at a flow rate of 0.2 mL/min. The eluents for the positive and negative polarity modes were eluent A (0.1% FA in Water) and eluent B (Methanol). The solvent gradient was set as follows: 2% B, 1.5 min; 2–85% B, 3 min; 85–100% B, 10 min; 100–2% B, 10.1 min; 2% B, 12 min. Q ExactiveTM HF mass spectrometer was operated in positive/negative polarity mode with spray voltage of 3.5 kV, capillary temperature of

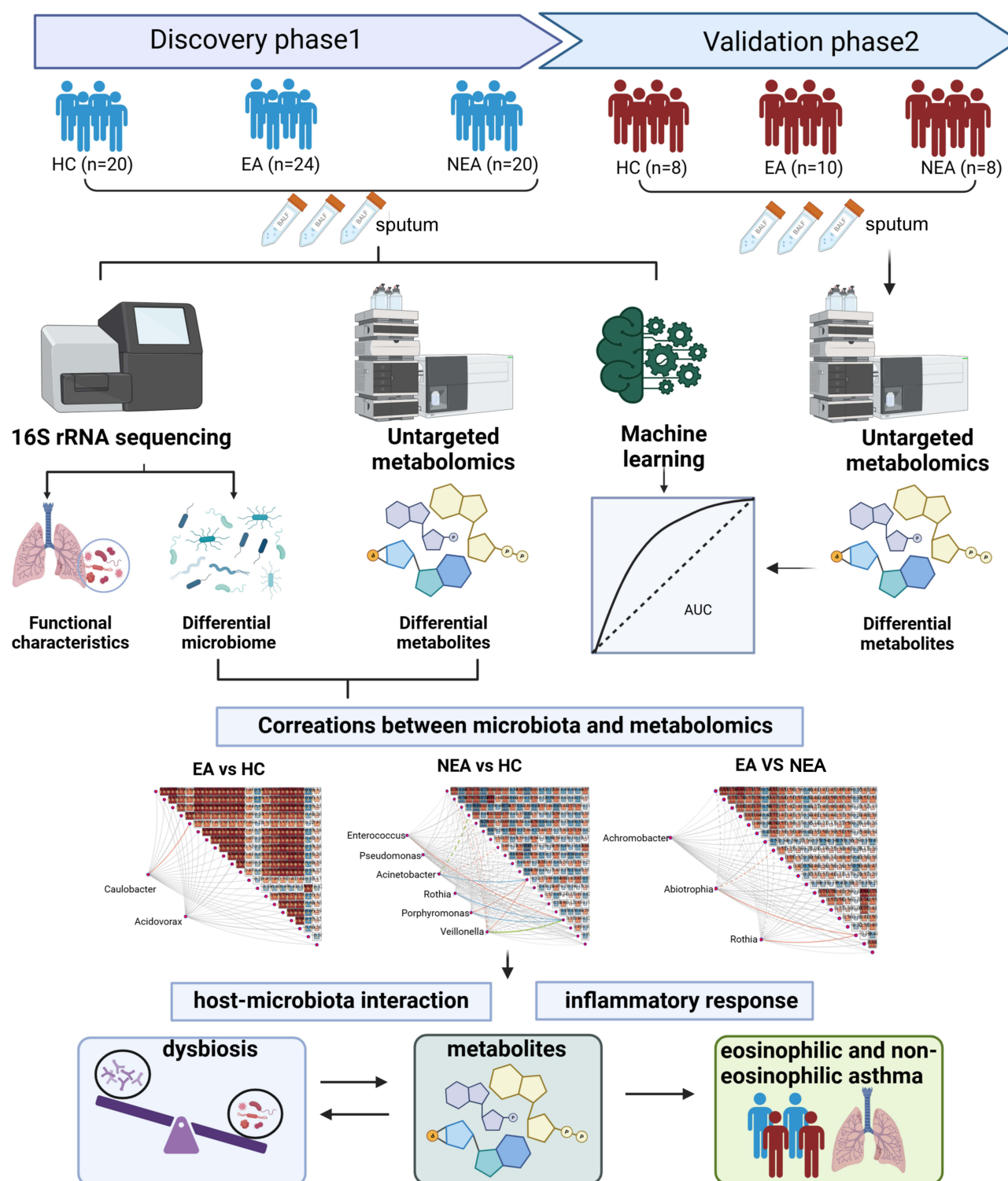


Figure 1 Visual representation of the study design. A cohort study combining microbiome analysis, metabolomics analysis, and machine learning applications to identify and validate biomarkers and pathways associated with asthma phenotypes and disease mechanisms.

320°C, sheath gas flow rate of 35 psi and aux gas flow rate of 10 L/min, S-lens RF level of 60, Aux gas heater temperature of 350°C. The raw data files generated by UHPLC-MS/MS were processed using the Compound Discoverer 3.3 (CD3.3, ThermoFisher) to perform peak alignment, peak picking, and quantitation for each metabolite.

Metabolomics Study

Principal component analysis (PCA) and orthogonal partial least squares-discriminant analysis (OPLS-DA) were used to explore whether all samples can be significantly clustered in different groups. We applied univariate analysis (*t*-test) to calculate the statistical significance (*P*-value). The metabolites with $VIP > 1$ and $P\text{-value} < 0.05$ and fold change ≥ 1.2 or $FC \leq 0.833$ were considered to be differential metabolites.^{28–30} Volcano plots were used to filter metabolites of interest which based on \log_2 (Fold Change), and $-\log_{10}(P\text{-value})$ of metabolites by ggplot2 in R language $P\text{-value} < 0.05$ was considered as statistically significant and correlation plots were plotted by corrplot package in R language. The functions of these metabolites and metabolic pathways were studied using the KEGG database.

Statistical Analysis

Statistical significance of the difference was firstly estimated using the F-test, followed by the Student's or Welch's *t*-test in two-group analysis according to the homogeneity of variance. Data normality was assessed by the Kolmogorov–Smirnov method. Comparisons between the two groups were performed by *t*-test with homogeneity of variance conversely. Mann–Whitney–Wilcoxon test was performed for the dataset, which does not follow the normality. Differences in airway bacteria diversity and relative abundance among three groups were analyzed by the nonparametric Kruskal–Wallis test. *P*-value of < 0.05 were considered statistically significant. All statistical analysis about the identification of distinct metabolites was completed with R (v4.0.2) basic statistical packages.

To evaluate the discriminatory power of classifiers in distinguishing between healthy controls and patients, the Receiver Operating Characteristic (ROC) Curve was employed. Based on the differential metabolites and microbiota obtained by the above analysis, ROC analysis was used to obtain curve and calculate the area under the curve (AUC), providing a quantitative measure of the model's performance. Furthermore, we ventured to enhance the predictive capability of our model by integrating the identified biomarkers.

Results

Characteristics of All Participants

Two cohorts were established to explore asthma heterogeneity based on induced sputum cytology: a discovery cohort with 44 asthma patients (24 with eosinophilic asthma, EA, and 20 with neutrophils asthma, NEA) and 20 healthy controls (HC), and a validation cohort consisting of 26 asthma patients (10 EA, 8 NEA) and 8 hC.

Baseline characteristics revealed no statistically significant differences in age, gender distribution, body mass index (BMI) across the groups. Serum total IgE levels were significantly higher in asthmatic patients compared to HC, with EA showing higher levels than NEA. Lung function analysis demonstrated significant intergroup differences: the percentages of FEV1 ($P = 0.018$), FEV1/FVC ratio ($P = 0.026$), and FVC ($P = 0.013$) were higher in the HC group than in both EA and NEA groups. Furthermore, these lung function indicators were higher in EA compared to NEA. EA exhibited significant eosinophilia in both blood and sputum, accompanied by lower neutrophil counts compared to NEA. NEA also had the longest hospital stay compared to the other groups. Clinical demographics of the discovery cohort are presented (Table 1), and the validation cohort showed high consistency with the discovery cohort (Table 2).

Microbiota in the Respiratory Tract of Different Asthma Patients versus HCs

Estimation of Sequencing Depth

To investigate these dynamics, 16S rRNA amplicon sequencing of sputum samples was performed to explore shifts in lung microbiota and uncover alterations in the structure and function of the lower respiratory tract microbiota. Based on Research statistics, raw 16S rRNA sequencing data using primers 515F and 806R were filtered using QIIME software, followed by sequence splicing with FLASH software to generate tag sequences. A total of 64 high-quality samples were obtained from sputum sequencing, with an average of 87,495 valid sequences per sample. At a 97% similarity threshold, 2696 Operational Taxonomic Units (OTUs) were identified. Rarefaction curves for each group indicated that sequencing data reached saturation, suggesting sufficient depth of coverage (Figure S2A). Rank abundance curves provided detailed insights into the richness and evenness of microbial diversity across the sample sets (Figure S2B). Additionally, the

Table 1 Clinical Parameters of Discovery Cohort

	Healthy Control	Eosinophilic Asthma (EA)	Neutrophils Asthma (NEA)	P
N	20	24	20	/
Age/year	43.5(38.5,54)	49(31,58.5)	53.5(47.5,62.5)	0.063
Gender (female/male)	11/9	13/11	14/6	0.511
BMI (kg/m ²)	23.99±2.89	23.65±2.87	21.68±3.62	0.117
Duration of Hospitalization	4.75±3.19	7.00±3.08	8.80±3.38	<0.01
Blood cell detections				
WBC, 10 ⁹ /L	6.00(4.37,7.06)	7.10(5.92,8.01)	8.81(6.46,10.75)	0.004
EOS, 10 ⁹ /L	0.15(0.08,0.22)	0.58(0.39,1.16)	0.20(0.11,0.44)	<0.001
NEU, 10 ⁹ /L	3.46(2.60,4.68)	3.65(2.62,4.17)	5.73(3.93,8.08)	0.002
LYM, 10 ⁹ /L	1.33(1.08,1.91)	2.09(1.79,2.70)	1.76(1.38,2.67)	0.005
PLT, 10 ⁹ /L	270.3±84.28	249.25±49.69	247.70±78.76	0.583
HGB, 10 ⁹ /L	127(120,144)	137(129.5,154)	127.5(122,142.75)	0.38
RBC, 10 ⁹ /L	4.56±0.41	4.80±0.59	4.53±0.57	0.195
EOS%	2.4(1.1,3.3)	10.2(5.78,14.15)	2.10(1.25,4.45)	<0.01
NEU%	61.21±11.62	49.85±11.12	63.16±11.30	<0.001
LYM%	26.98±10.56	31.58±8.40	25.45±10.30	0.099
Sputum				
Neutrophils %	47.5(41.75,85.63)	43.38(22.38,62.38)	94.13(81.25,97.38)	<0.01
Eosinophils %	0.25(0,1.75)	40.75(13.88,55.44)	0.75(0,1.38)	<0.01
Macrophages %	45.5(9.13,52.38)	12.88(4.63,21.00)	3.75(1.63,18.25)	0.051
Lymphocytes %	2.50(0.88,10.63)	0.50(0,1.50)	0.50(0,1.50)	0.069
Lung function				
FEV1/FVC	84.55(82.85,84.9)	83.63(83.22,84.04)	83.97(83.86,84.20)	0.026
FEV1	2.92(2.30,3.45)	2.78(2.77,3.17)	2.40(2.07,2.80)	0.018
FVC	3.55±0.62	3.11±0.64	2.91±0.77	0.013
Inflammatory indicators				
IgE, mg/L	65.86(26.20,99.1)	174.11(91.80,490.2)	98.87(45.47,231.48)	0.017

Abbreviations: WBC, White blood cell; EOS, Eosinophils; NEU, Neutrophil; LYM, Lymphocyte; PLT, Blood platelet; HGB, Glycosylated hemoglobin; RBC, Red blood cell; FEV1, Forced expiratory volume in one second; FVC, Forced vital capacity; IgE, Total IgE.

species accumulation boxplot demonstrated a steady increase in species diversity as sample size increased, with curves plateauing at the maximum sample size of 64, further supporting the adequacy of sequencing depth ([Figure S2C](#)).

Alpha-Diversity and Beta-Diversity

Alpha-diversity was assessed to analyze microbial community diversity within individual groups. Metrics such as Chao1, Shannon Diversity, Simpson, and Richness indices did not reveal significant differences in species richness or diversity, indicating that α -diversity remained consistent across the three study groups ($P > 0.05$, Kruskal–Wallis tests) ([Figure 2A](#)). In contrast, beta-diversity, which compares microbial community composition across different groups, demonstrated significant differences between EA and NEA ($P = 0.03$, Wilcoxon test, unweighted UniFrac distance), and between NEA and HC ($P = 9e-04$, Wilcoxon test, unweighted UniFrac distance) ([Figure 2B](#)). These findings were supported by the Principal Coordinates Analysis (PCoA) plot, which illustrated shifts in microbial community composition among the groups ([Figure S1A](#)). The PCoA, based on Bray–Curtis dissimilarities, highlighted statistically significant differences in overall microbiota structure between HC and NEA, as well as between EA and NEA. Non-metric multidimensional scaling (NMDS) analysis, based on Bray–Curtis similarity distance, further demonstrated distinct group separation (stress

Table 2 Clinical Parameters of Validation Cohort

	Healthy Control	Eosinophilic Asthma (EA)	Neutrophils Asthma (NEA)	P
N	8	10	8	/
Age/year	47(25,52.75)	55(46,59)	51(34,62)	0.316
Gender (female/male)	5/3	8/2	6/4	0.599
BMI (kg/m ²)	23.32±3.34	22.96±1.92	23.65±3.17	0.865
Duration of Hospitalization	5.00(1.75,7.50)	7.50(6.00,8.00)	8.00(5.50,9.25)	0.033
Blood cell detections				
WBC, 10 ⁹ /L	7.08(6.63,9.28)	6.78(6.23,8.44)	7.83(6.63,10.09)	0.006
EOS, 10 ⁹ /L	0.18(0.08,0.22)	0.72(0.27,0.78)	0.14(0.11,0.20)	0.006
NEU, 10 ⁹ /L	3.67(3.13,5.08)	3.05(2.53,4.20)	4.68(3.92,7.31)	0.019
LYM, 10 ⁹ /L	1.43±0.63	1.83±0.37	2.61±0.32	<0.001
PLT, 10 ⁹ /L	278.88±55.04	240.38±33.42	272.22±60.00	0.292
HGB, 10 ⁹ /L	134.13±12.71	129.25±15.56	131.11±18.20	0.826
RBC, 10 ⁹ /L	4.74±0.34	4.32±0.59	4.64±0.68	0.29
EOS%	2.45(1.35,3.38)	10.90(4.5,16.58)	2.10(1.40,2.80)	0.006
NEU%	61.94±11.48	47.27±9.78	59.77±10.89	0.025
LYM%	23.94±7.09	31.60±5.74	28.63±9.20	0.148
Sputum				
Neutrophils %	46.5(41.55,86.20)	35.00(12.63,50.50)	87.50(83.50,96.00)	<0.001
Eosinophils %	0.3(0, 1.85)	36.25(12.31,65.38)	0.50(0.00,1.00)	<0.001
Macrophages %	40.5(7.52, 52.56)	23.08±15.88	8.46±7.15	0.059
Lymphocytes %	1.75(0.88, 8.26)	0.63(0.00,1.94)	0.25(0.00,0.50)	0.192
Lung function				
FEV1/FVC	85.48(83.97,87.8)	83.49(78.20,84.03)	83.99(83.83,84.34)	0.028
FEV1	2.76±0.41	2.25±0.30	2.14±0.39	0.016
FVC	3.16±0.97	2.16±0.51	1.94±0.43	0.005
Inflammatory indicators				
IgE, mg/L	33.99(6.74,80.30)	174.58(58.79,203.9)	81.16(50.54,195.73)	0.031

Abbreviations: WBC, White blood cell; EOS, Eosinophils; NEU, Neutrophil; LYM, Lymphocyte; PLT, Blood platelet; HGB, Glycosylated hemoglobin; RBC, Red blood cell; FEV1, Forced expiratory volume in one second; FVC, Forced vital capacity; IgE, Total IgE.

= 0.089, [Figure S1B](#)). A Venn diagram ([Figure 2C](#)) visually depicted the shared and unique OTUs among the groups, providing insights into their compositional differences.

Distribution of Microbiota Taxonomic Composition in Different Asthma Patients

All sequences were classified into 30 phyla. The relative abundance of the top 10 phyla across the three groups is displayed in [Figure 2D](#). The most abundant phyla in the airway microbiota were *Proteobacteria*, *Firmicutes*, *Bacteroidetes*, and *Fusobacteriota*. EA patients exhibited a higher abundance of the *Proteobacteria* phylum, while NEA patients showed higher abundances of *Bacteroidetes*, *Aenigmarchaeota*, and *Firmicutes*. However, there were no significant differences in phylum-level distribution between HC and asthma patients ($P > 0.05$, MetagenomeSeq, [Figure 2E](#)). Despite similar phylum-level distributions, genus-level analysis revealed distinct patterns. Both healthy controls and asthma patients shared four major bacterial genera: *Stenotrophomonas*, *Streptococcus*, *Achromobacter*, and *Neisseria*. Notably, *Veillonella* was more abundant in NEA patients compared to HC, while *Achromobacter* was more prevalent in NEA patients than in EA patients ($P < 0.05$, MetagenomeSeq, [Figure 2F](#)). These results underscore the nuanced differences in microbial composition at the genus level, despite similarities at the broader phylum level.

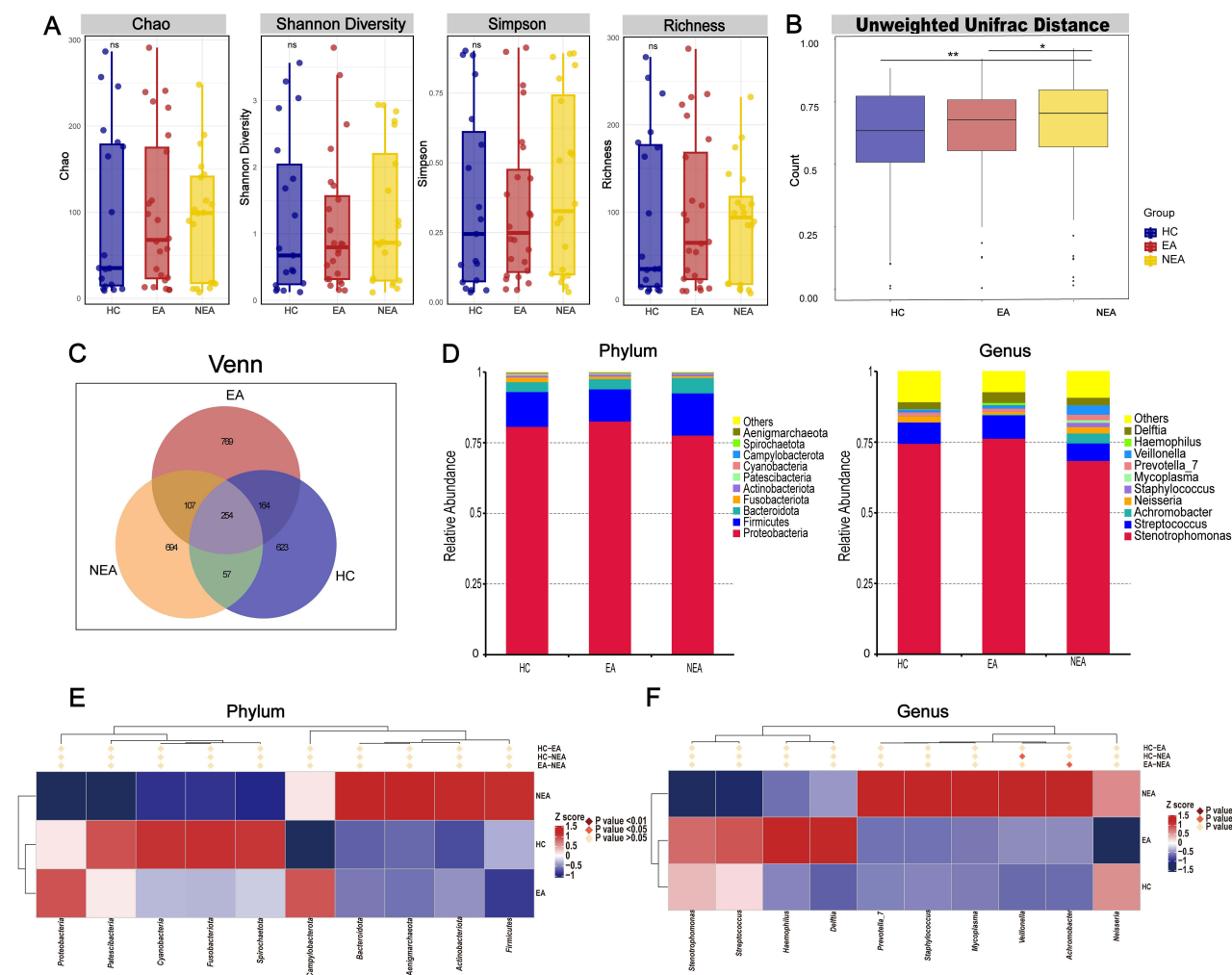


Figure 2 Characteristics of the airway microbiome composition. **(A)** Alpha diversity analysis. **(B)** Microbial community beta-diversity. **(C)** Venn diagram of OTUs. **(D)** Relative abundance of top 10 phylum and genus. **(E)** Heatmap of microbial relative abundances of top 10 phylum. **(F)** Heatmap of microbial relative abundances of top 10 genus. * $P < 0.05$, ** $P < 0.01$.

Altered Composition of the Respiratory Tract in Different Asthma Patients

We utilized the MetagenomeSeq method to identify genus-level taxa with significant statistical and biological differences among the three groups. In the comparison between EA and HC, *Caulobacter* and *Acidovorax* were more abundant in EA than in HC ($P < 0.05$, Figure 3A). In the comparison between NEA and HC, a marked enrichment of *Enterococcus*, *Pseudomonas*, *Acinetobacter*, *Rothia*, *Porphyromonas*, and *Veillonella* was observed in the NEA group ($P < 0.05$, Figure 3B). Further comparison between EA and NEA revealed that *Achromobacter*, *Abiotrophia*, and *Rothia* were more abundant in NEA compared to EA ($P < 0.05$, Figure 3C). This differential abundance pattern highlights the unique microbial landscapes characterizing EA and NEA, which may contribute to their distinct clinical manifestations and disease mechanisms.

With the confirmation of airway microbial dysbiosis among the patients, we next explored the potential of the airway microbiota as diagnostic indicators. Using random forest analyses, we sought to identify taxonomic markers that could distinguish between EA and HC, as well as between NEA and the other two groups. This analysis constructed a random forest predictive model based on OTU feature selection. By selecting general with the highest area under the curve (AUC) values, we identified key markers (Figure S3). For distinguishing EA from HC, five general were selected based on MeanDecreaseAccuracy (Figure 3D), and a 10-fold cross-validation was applied. ROC curves were plotted to evaluate predictive performance, yielding an AUC of 66.78%, indicating moderate discriminatory ability (Figure 3E). However,

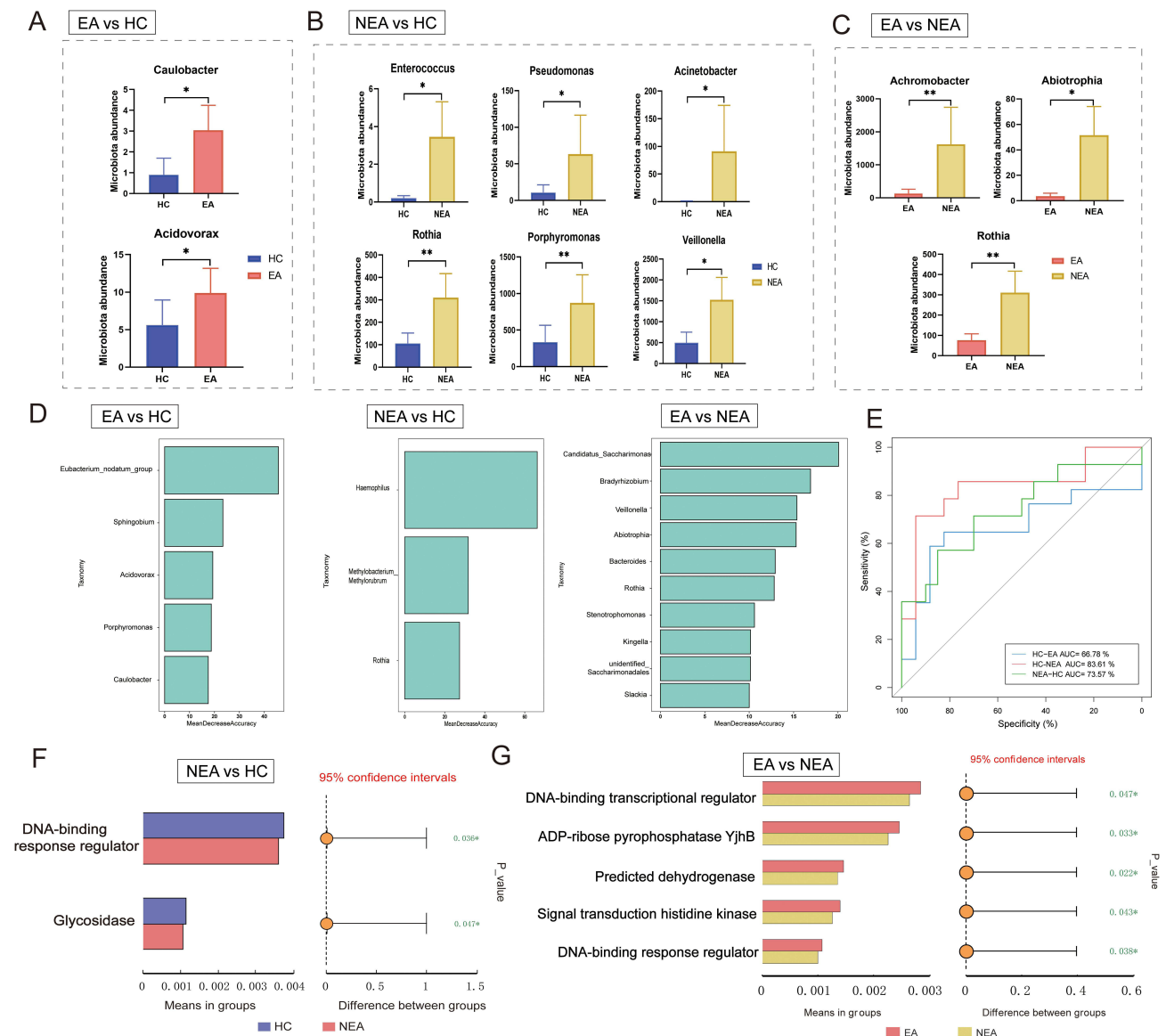


Figure 3 Prediction model of airway microbiota for EA and NEA based on genus-level abundances using random forests. (A–C) Genus-level taxa differed between groups. (D) Variable importance ranking chart. (E) ROC curve of the model. (F) COG functional analysis of microbiota between NEA and HC. (G) COG functional analysis of microbiota between EA and NEA. * $P < 0.05$, ** $P < 0.01$.

the model demonstrated robust performance in distinguishing NEA from both HC and EA. Remarkably, only three general were required to achieve the highest AUC value of 83.81% when distinguishing NEA from HC, underscoring strong discriminatory potential. These findings suggest that the airway microbiota holds significant promise as a diagnostic tool, particularly in identifying NEA patients from healthy controls. Additionally, *Haemophilus*, *Methylobacterium*, and *Rothia* emerged as potential biomarkers for identifying individuals predisposed to developing neutrophils asthma.

Functional predictions of microbial communities based on 16S rRNA gene sequences were conducted using PICRUSt2 with the COG database. Distinct functional categories within the COG database were identified between NEA and HC groups, reaching statistical significance ($P < 0.05$, Figure 3F), including DNA-binding response regulators and glycosidases. A comparative analysis between EA and NEA microbial communities also revealed statistically significant differences ($P < 0.05$, Figure 3G) in five key functional domains, including DNA-binding transcriptional regulators, ADP-ribose pyrophosphatase Yjhb, predicted dehydrogenase, signal transduction histidine kinase, and DNA-

binding response regulators. These functional differences provide valuable insights into the structure and functionality of microbial communities and their interactions under distinct environmental conditions.

Metabolomics Analysis of Different Asthma Patients versus HC

Multivariate Analysis of Metabolomic Data

To further elucidate the pathogenesis of asthma in different patient subtypes, residual sputum samples were analyzed for metabolomics. In positive ion mode (ESI+), 807 metabolites were identified, with 252 annotated against the KEGG database. In negative ion mode (ESI-), 532 metabolites were identified, with 193 annotated. The PCA score plots in both 2D and 3D for the sputum metabolome in ESI+ and ESI- modes ([Figure S4A](#) and [B](#)) demonstrated strong stability across samples in both ionization modes, confirming the reliability of the metabolomic system. A clear segregation was observed between EA, NEA, and HC groups, indicating significant metabolic differences. Each sample was represented as a point on the score plots, and permutation tests ($n = 200$) were used to validate the OPLS-DA model. The permutation plots showed that all blue Q2-values to the left were lower than the original points on the right, confirming the validity of the models. OPLS-DA clearly separated metabolites between the groups under investigation ([Figure S4C–H](#)), highlighting distinct metabolic profiles across asthma subtypes.

Identification of the Differential Metabolites in Sputum

A combined analysis of positive and negative ions was conducted to comprehensively understand metabolite functions. Metabolites that distinguished asthma patients from controls were selected based on fold change (cutoff >1.2 or <0.833) and VIP scores from OPLS-DA.

A total of 269 metabolites showed significant differences between EA patients and HC ([Figure 4A, D, G](#)), with 180 metabolites upregulated and 89 downregulated in EA patients ($VIP > 1$, $P < 0.05$). Notably, lipids and lipid-like molecules such as 15(S)-HpETE, Lipoxin B4, and 15-Epiprostaglandin E1 were elevated in EA patients, while glycerophospholipids such as Thymidine 5'-monophosphate and Uridine monophosphate (UMP) were downregulated.

For NEA patients, 224 metabolites exhibited significant differences compared to HC ([Figure 4B, E, H](#)), with 149 metabolites upregulated and 75 downregulated ($VIP > 1$, $P < 0.05$). Notable metabolites in NEA included elevated levels of PC 16:0_16:1 and D-Raffinose, while methadone-d9 and 2-Methylglutaric acid were downregulated. In the comparison between EA and NEA groups, 166 metabolites showed significant differences in relative abundance ([Figure 4C, F, I](#)), with 88 upregulated and 78 downregulated in EA patients ($VIP > 1$, $P < 0.05$). Key metabolites such as 5-Hydroxymethyluracil, methadone-d9, and 5-Hydroxyindole-3-acetic acid were elevated in EA patients, while Quinolinic acid and PC 16:0_16:1 was downregulated in NEA patients.

Enrichment Analysis and Correlation of Metabolites in Sputum

The Kyoto Encyclopedia of Genes and Genomes (KEGG) database provides a comprehensive resource for the functional interpretation of genomes and high-throughput data generated from large-scale experimental technologies. The altered metabolites in this study were primarily associated with amino acid and lipid metabolism. In the comparison between EA and HC, the significantly different metabolites were enriched in 51 metabolic pathways, with three pathways showing significant differences: pyrimidine metabolism, phenylalanine metabolism, and bile secretion ($P < 0.05$) ([Figure 5A](#)). For NEA versus HC, 46 pathways were identified, with four showing significant differences, including tryptophan metabolism, protein digestion and absorption, and phenylalanine metabolism ($P < 0.05$) ([Figure 5B](#)). In the comparison between EA and NEA, 38 pathways were enriched, with four pathways showing significant differences, including arachidonic acid metabolism, pyrimidine metabolism, serotonergic synapse, and leishmaniasis ($P < 0.05$) ([Figure 5C](#)).

Correlation analysis helps to elucidate the synergistic or mutually exclusive relationships between different metabolites, providing insight into their regulatory interactions during biological state changes. A heat map of the top 20 differential metabolites between EA and HC shows that most lipids and lipid-like molecules were positively correlated ([Figure 5D](#)). In the comparison between NEA and HC, 5-hydroxyindole-3-acetic acid, derived from indoles and derivatives, showed a positive correlation with 5-hydroxymethyluracil, derived from diazines, while no strong correlations were observed among other metabolites ([Figure 5E](#)). In the EA versus NEA comparison, fatty acyls such as 5(S),15

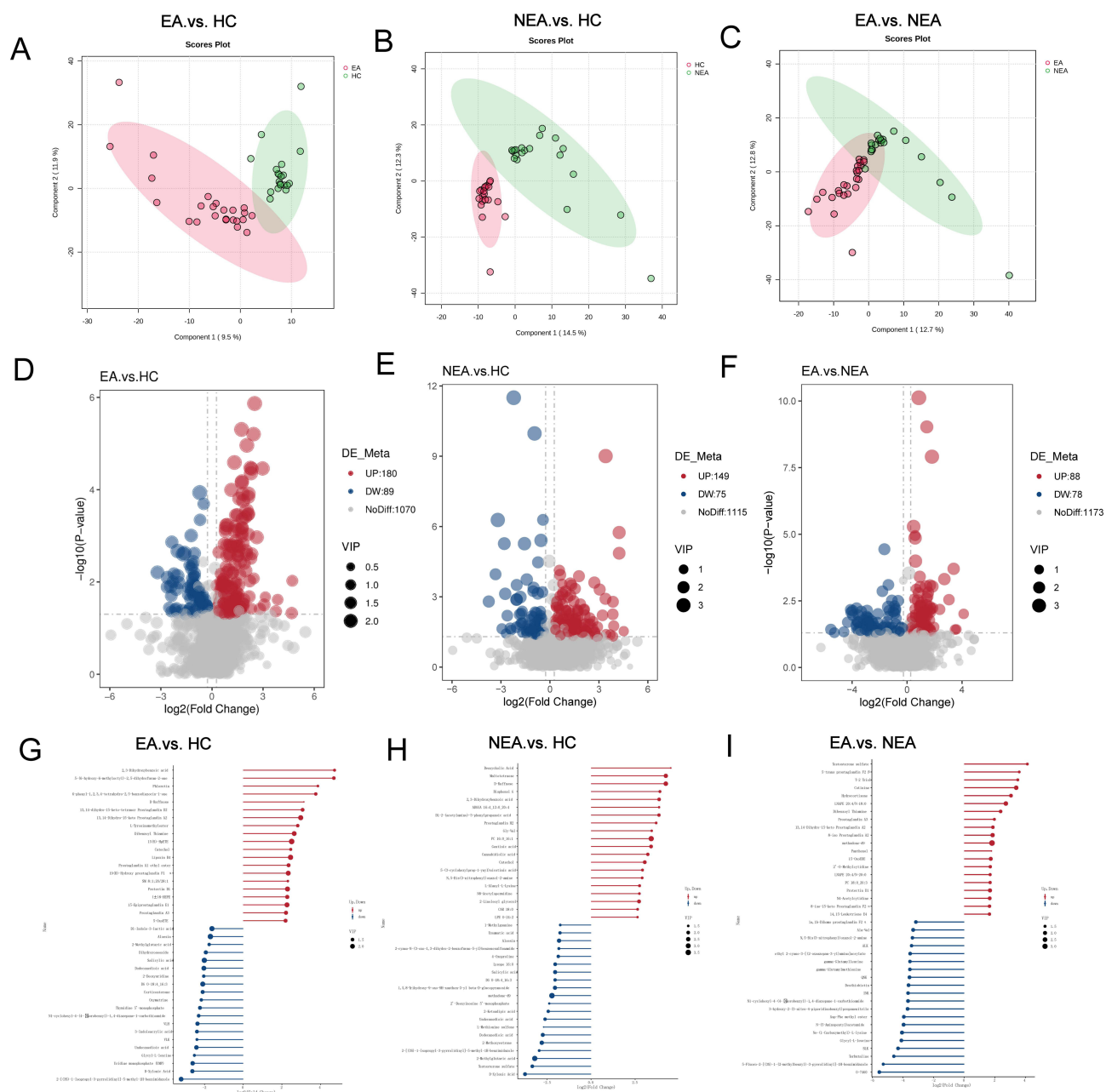


Figure 4 Metabolic profiles among three groups. (A–C) PLS-DA plot for pairwise comparison between groups (D–F) Volcano plot of metabolites of pairwise comparison between groups. (G–I) Matchstick chart of the top 20 different metabolites between EA and HC, NEA and HC, EA and NEA.

(S)-DiHETE exhibited positive correlations with Protectin D1, a lipid mediator with anti-inflammatory and immunoregulatory effects (Figure 5F). The positive correlation between these two metabolites may suggest a shared inflammatory response or immunoregulatory mechanism between the EA and NEA groups.

Random Forest Analysis Discovered Potential Metabolic Biomarkers for Asthma Patients' Stratification

In the comparison between EA and HC, KEGG enrichment analysis identified three significantly different pathways—pyrimidine metabolism, phenylalanine metabolism, and bile secretion ($P < 0.05$). Among these, pyrimidine metabolism had the smallest P-value, indicating the highest reliability. Consequently, we established a random forest model based on the eight differential metabolites enriched in the pyrimidine metabolism pathway to identify metabolic biomarkers capable of distinguishing EA from HC. The mean decrease Gini score highlighted the prominent metabolites

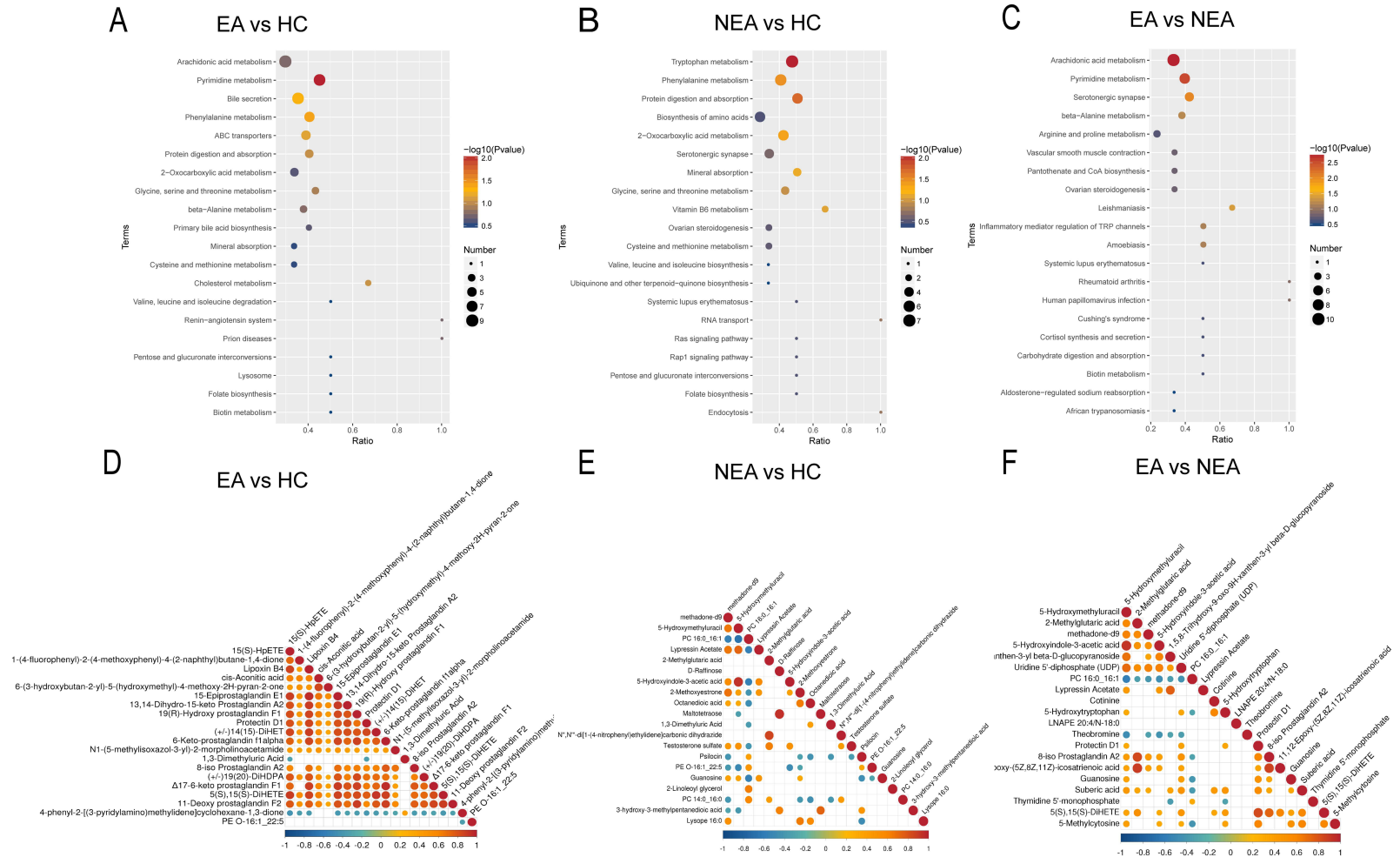


Figure 5 Enrichment Analysis and correlation of metabolites in sputum. (A–C) KEGG pathway enrichment analysis of the top 20 differential metabolites between EA and HC, NEA and HC, EA and NEA. (D–F) Correlation analysis of the top 20 differential metabolites between EA and HC, NEA and HC, EA and NEA.

differentiating EA from HC (Figure 6A). The top metabolites associated with EA included methylmalonate, 5-methylcytosine, dUDP, and 2-deoxyuridine (Figure 6B). To enhance the accuracy of biomarker identification, these four metabolites were combined in a ROC analysis, achieving an AUC of over 0.90, significantly higher than that of individual metabolites (Figure 6C).

In the comparison between NEA and HC, tryptophan metabolism exhibited the smallest P-value. We developed a random forest model using the seven differential metabolites enriched in the tryptophan metabolism pathway to identify biomarkers distinguishing NEA from HC (Figure 6D). The top metabolites associated with NEA included quinolinic acid, 5-hydroxyindole-3-acetic acid, acetyl-N-formyl-5-methoxykynurenamine, and 2-ketoadipic acid (Figure 6E), with a combined AUC of 0.90 in the test set (Figure 6F).

In the comparison between EA and NEA, the arachidonic acid metabolism pathway showed the most significant P-value. A random forest model was established with nine differential metabolites from this pathway to identify metabolic biomarkers distinguishing EA from NEA (Figure 6G). The top metabolites associated with NEA included prostaglandin E2, 15(S)-HpETE, PC 34:1, PC 32:0, and 11,12-epoxy-(5Z,8Z,11Z)-icosatrienoic acid. The expression of these metabolites in each group is shown in Figure 6H, with a combined AUC of 0.93 in the test set (Figure 6I).

To further validate the metabolites identified through non-targeted metabolomics, an external validation cohort was analyzed. Consistent with the discovery cohort results, significant differences were observed, particularly in the comparison between EA and HC. The four metabolites involved in pyrimidine metabolism—methylmalonate, 5-methylcytosine, dUDP, and 2-deoxyuridine—showed consistent high AUC results in the validation cohort. Additionally, using these four metabolites to differentiate NEA from HC achieved an AUC of 0.91 in the validation set, demonstrating excellent diagnostic performance. Similar findings were confirmed in comparisons between EA and NEA (Figure 6J).

Correlation Between Airway Microbiome and Metabolites

To investigate the relationship between the altered airway microbiome and metabolites involved in asthma pathogenesis, we calculated Spearman correlation between differential bacteria and the top 40 differential metabolites across the different groups. In the comparison between EA and HC, we found that the *Caulobacter* genus positively correlated with the metabolite 6-(3-hydroxybutan-2-yl)-5-(hydroxymethyl)-4-methoxy-2H-pyran-2-one, though no specific functional annotation was available in KEGG (Figure 7A).

In the comparison between NEA and HC, all six different general exhibited positive correlations with metabolites (Figure 7B). Notably, *Veillonella*, *Acinetobacter*, *Pseudomonas*, and *Enterococcus* were positively associated with LPE 18:0, 2-linoleoyl glycerol, and cis-aconitic acid. LPE 18:0 and 2-linoleoyl glycerol are lipids and lipid-like molecules, while cis-aconitic acid is an organic acid involved in the 2-oxocarboxylic acid metabolism pathway. The *Porphyrromonas* genus correlated positively with salicylic acid, a benzenoid involved in the phenylalanine metabolism pathway. The *Rothia* genus correlated positively with metabolites such as N⁺, N⁺-di[1-(4-nitrophenyl)ethylidene]carbonic dihydrazide, 1-(4-fluorophenyl)-2-(4-methoxyphenyl)-4-(2-naphthyl)butane-1,4-dione, and dihydrothymine, while showing negative correlations with Lyppressin acetate and 2-methoxyestrone.

In the comparison between EA and NEA, interesting correlations were observed between specific bacterial general and distinct metabolites. *Abiotrophia* and *Achromobacter* general exhibited a positive correlation with thymidine 5'-monophosphate, a nucleoside involved in the antifolate resistance pathway (Figure 7C). The *Abiotrophia* genus also showed a negative correlation with 3-methyluridine, another nucleoside. *Achromobacter* positively correlated with (±) 9-HpODE, suggesting a potential link between this genus and specific lipid peroxidation products. Additionally, *Rothia* correlated positively with N1-cyclohexyl-4-(4-fluorobenzyl)-1,4-diazepane-1-carbothioamide. These findings highlight the intricate interplay between airway microbial communities and their metabolic byproducts in different asthma phenotypes, potentially contributing to the heterogeneity observed in asthma pathogenesis. Additionally, we compared the correlations between differentially microbial/metabolites and granulocyte percentages in EA and NEA. The correlation analysis revealed that *Abiotrophia* positively correlated with sputum neutrophils. *Achromobacter* showed strong associations with blood neutrophil counts (Figure S5A). These findings support EA and NEA as distinct endotypes, with *Abiotrophia* and *Achromobacter* linked to neutrophilic inflammation. The differential metabolites 15(S)-HpETE and 11,12-Epoxy-(5Z,8Z,11Z)-icosatrienoic acid exhibited significant positive correlations with eosinophils in both sputum

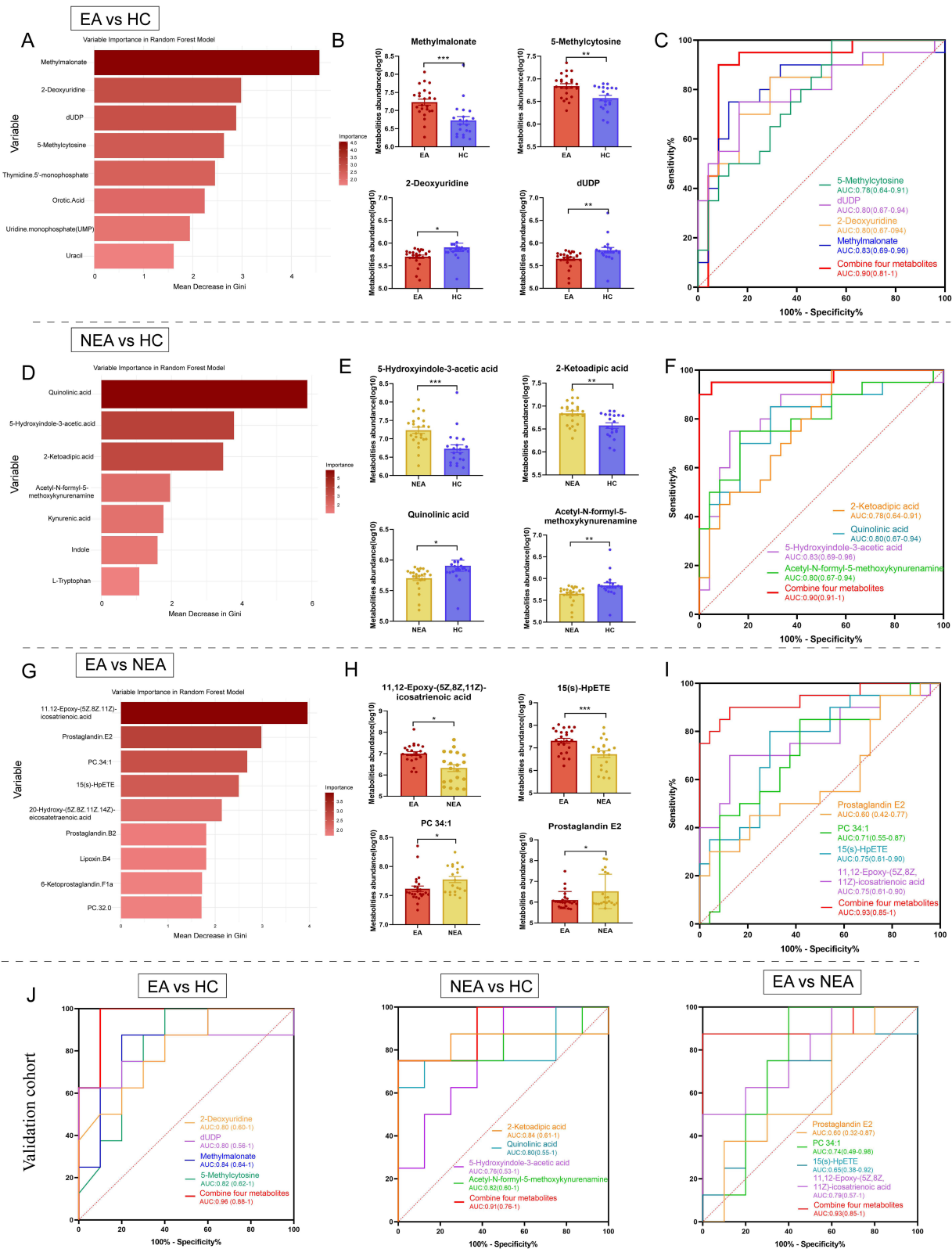


Figure 6 Metabolic markers of EA and NEA by random forest models. (A–C) Candidate metabolites classifying EA and HC. (D–F) Candidate metabolites classifying NEA and HC. (G–I) Candidate metabolites classifying EA and NEA. (J) ROC curve analysis of the candidate biomarkers.

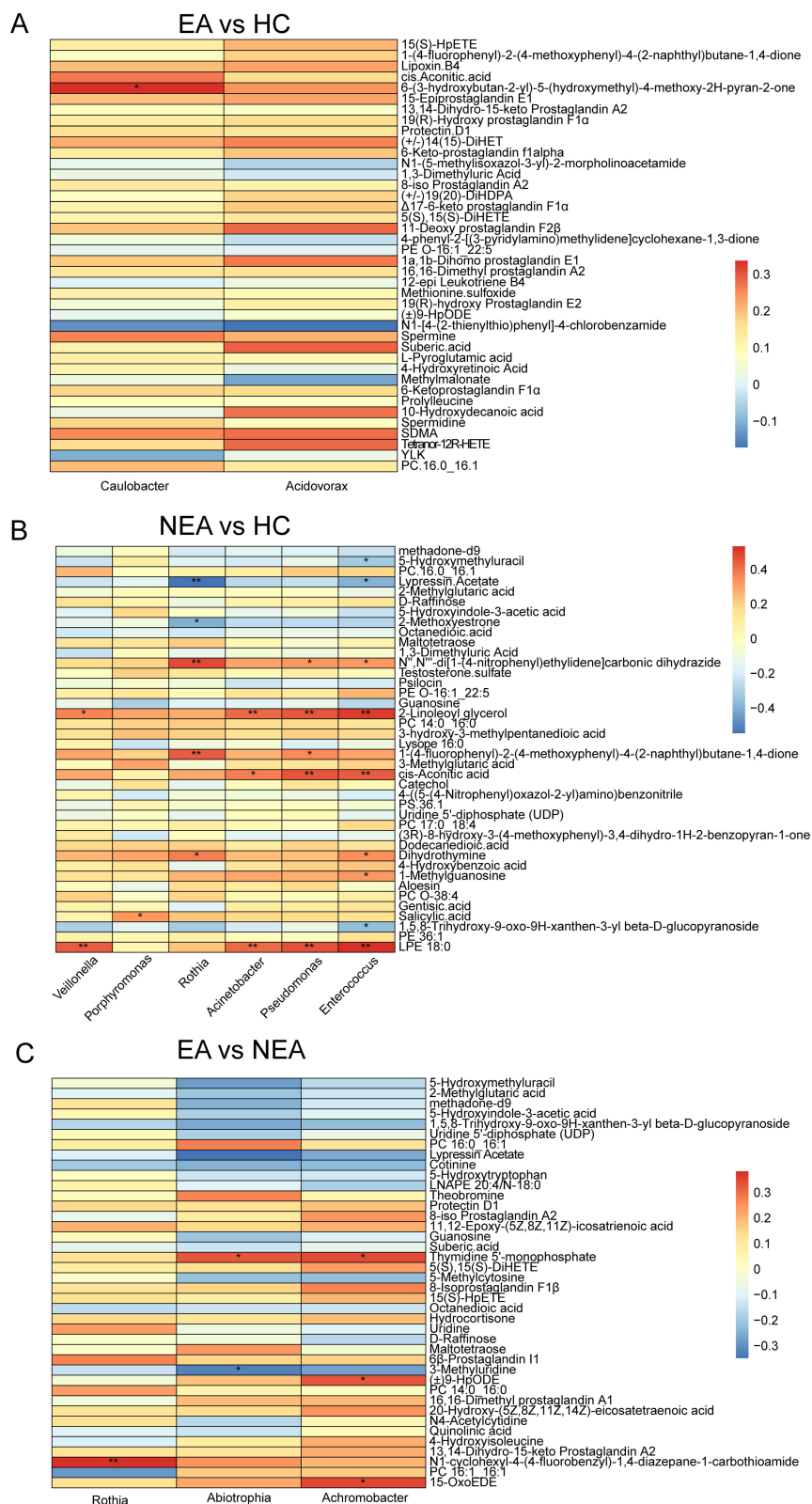


Figure 7 Spearman correlation heatmap for significantly altered metabolites and general among the three groups. **(A)** Correlation heatmap between EA and HC. **(B)** Correlation heatmap between NEA and HC. **(C)** Correlation heatmap between EA and NEA. * $P < 0.05$, ** $P < 0.01$.

and blood (Figure S5B). The compartment-specific (sputum vs blood) and phenotype-dependent patterns highlight potential biomarkers for targeted therapies.

Discussion

This study highlights the pivotal role of the lower airway microbiota in asthma pathogenesis, aligning with the growing body of research on the microbiome's influence on asthma outcomes.^{12,31,32} By integrating 16S rRNA sequencing with untargeted metabolomics, we sought to uncover distinct microbial and metabolic signatures across EA, NEA, and HC, advancing our understanding of asthma's heterogeneity.

At the phylogenetic level, our study provides robust evidence for the existence of a core respiratory microbiome, comprising *Proteobacteria*, *Firmicutes*, *Bacteroidota*, and *Fusobacteriota*, which serves as a foundational component of respiratory health across both healthy individuals and those with asthma. This core microbiome underscores the critical role of these microbial groups in maintaining respiratory homeostasis, regardless of asthma status. However, genus-level differences revealed significant shifts in microbial composition, particularly between EA and NEA. The enrichment of *Caulobacter* and *Acidovorax* in EA suggests these genera may contribute to eosinophilic inflammation.^{33,34} The presence of these bacteria may influence the local immune response, promoting the recruitment and activation of eosinophils, which are central to the inflammatory process in EA. While the increased abundance of *Enterococcus*, *Pseudomonas*, *Acinetobacter*, *Rothia*, *Porphyromonas*, and *Veillonella* in NEA reflects a microbial signature commonly associated with infection and inflammation. This microbial signature is commonly associated with infection and inflammation, indicating a potential role for these bacteria in driving the inflammatory pathways characteristic of NEA.

Functionally, the identification of two significantly altered classes—DNA-binding response regulators and glycosidases—between NEA and HC underscores the profound impact of NEA on cellular processes. DNA-binding proteins, as transcriptional regulators, influence gene expression related to inflammation, immune responses, and cell proliferation.³⁵ Similarly, glycosidases, which are key enzymes involved in glycan processing, also exhibit significant alterations in NEA. This suggests that NEA may disrupt the normal glycan metabolism, further illustrating the complexity of cellular changes associated with this asthma subtype.³⁶ The interplay between glycosidases and other cellular components may be crucial in understanding the pathogenesis of NEA and developing targeted therapeutic strategies.³⁷ In addition, the significant differences in five functional categories, including transcriptional regulators, ADP-ribose pyrophosphatase Yjhb, predicted dehydrogenases, signal transduction histidine kinases, and DNA-binding response regulators, between EA and NEA, span a wide range of metabolic and regulatory processes, reflecting the sophisticated nature of microbial interactions within each asthma phenotype. These findings reveal the sophisticated nature of the microbial interactions within each phenotype and the need for targeted therapeutic strategies to address their distinct pathogenic mechanisms.

Our metabolomics analysis revealed significant metabolic differences between EA and NEA, providing new molecular-level evidence for understanding the heterogeneity of asthma. In EA, the upregulation of pro-inflammatory lipids such as 15(S)-HpETE and lipoxin B4 is highly consistent with the previously reported Th2-type inflammatory characteristics in the airways.³⁸ The downregulation of nucleic acid precursors such as thymidine 5'-monophosphate and UMP reflects metabolic reprogramming in airway epithelial cells under chronic inflammatory conditions, aligning with the mitochondrial dysfunction observed in EA patients.³⁹ NEA exhibits distinct metabolic features: the increase in PC 16:0_16:1 may affect airway smooth muscle reactivity by altering cell membrane fluidity, a mechanism validated in the lipidomics study.⁴⁰ Meanwhile, the downregulation of methadone-d9 and 2-methylglutaric acid may indicate NEA-specific tryptophan metabolism disorders. These findings deepen our understanding of asthma endotyping: EA is dominated by arachidonic acid metabolism, whereas NEA involves phospholipid remodeling and microbial co-metabolism, establishing a robust biochemical basis for the clinical and immunological differences between these two major asthma endotypes.

In EA, altered pyrimidine metabolism was among the most significantly affected pathways, indicating its role in regulating inflammatory responses and cellular proliferation.⁴¹ Altered pyrimidine metabolism played a key role, with four metabolites (Methylmalonate, 5-Methylcytosine, dUDP, 2-Deoxyuridine) identified as robust biomarkers. In NEA, alterations in tryptophan metabolism were the most significant, suggesting that modulation of this pathway may be key to understanding NEA-associated metabolic changes. Tryptophan breakdown products play crucial roles in the synthesis of

bioactive compounds like serotonin and melatonin, which influence immune function, mood, and sleep regulation.^{42,43} Additionally, the involvement of protein digestion and absorption pathways in NEA indicates possible disruptions in nutrient processing, further highlighting its metabolic complexity. Biomarkers for NEA, including quinolinic acid, 5-hydroxyindole-3-acetic acid, acetyl-N-formyl-5-methoxykynurenamine, and 2-ketoadipic acid, demonstrated strong predictive value. Arachidonic acid metabolism distinguished EA and NEA, with potential therapeutic targets identified.^{44,45} Altered arachidonic acid metabolites in allergic rhinitis serum suggested a metabolic association.¹⁶ The consistency of these metabolic markers across validation cohorts strengthened their reliability and clinical significance. Overall, these findings provided insights into metabolic pathways and biomarkers for targeted therapies and diagnostics.

In exploring the link between airway microbiota alterations and metabolite changes in disease pathogenesis, our Spearman correlation analysis revealed intriguing findings. The airway microbiota may impact the host's metabolic state, influencing asthma onset and inflammation development. Comparisons showed broader microbe-metabolite correlations in EA vs HC, with specific general correlated with lipids. In asthmatics with EA vs NEA, different general were linked to nucleoside metabolism and other pathways. These results suggest microbial communities influence disease progression by modulating metabolic pathways, potentially affected by microbiota structure and nutritional homeostasis. Additionally, we also investigated how the differential microbial communities and metabolites correlate with granulocyte levels in EA and NEA. Although no statistically significant correlations were observed between the differential microbial communities and neutrophil levels in sputum or blood, likely due to the small sample size and the low abundance of the differentially abundant microbial taxa, a positive correlation trend was still noticeable. This suggests that airway microbial dysbiosis may primarily be involved in neutrophil-dominated inflammatory pathways in asthma, whereas key metabolites are mainly positively correlated with eosinophils in both blood and sputum, with lipid mediators orchestrating systemic recruitment of eosinophils. For instance, the 15(S)-HpETE and epoxy fatty acid metabolic pathways, known to modulate type 2 inflammation,⁴⁶ have been implicated, thereby revealing important mechanistic links between microbial/metabolic features and granulocyte-driven inflammation in asthma phenotypes.

Our multi-omics approach has offered novel insights into complexities of asthma, particularly by highlighting differences in airway microbial communities, functional characteristics, and metabolic pathways between EA and NEA. However, the journey toward identifying robust biomarkers for asthma stratification and personalized treatment is fraught with challenges, such as sample size limitations and methodological variability persist, necessitating further validation in larger cohorts to confirm reproducibility and clinical utility. Despite these limitations, our study represents a crucial step toward personalized asthma treatment, laying the foundation for targeted strategies. Future research should focus on elucidating the causal mechanisms underlying microbiome-metabolite interactions in asthma to identify robust biomarkers for more precise and effective management.

Conclusion

This study highlights the profound differences in airway microbial community structure, functional characteristics, and metabolite levels between eosinophilic asthma, neutrophils asthma, and healthy controls. By integrating 16S rRNA sequencing, metabolomics analysis, and the random forest algorithm, we have gained significant insights into the pathogenesis of asthma. This comprehensive approach not only enhances our understanding of the disease's complexity but also lays a foundation for advancing personalized approaches in asthma care, facilitating more precise and targeted disease characterization and monitoring.

Abbreviations

EA, Eosinophilic asthma; NEA, Neutrophils asthma; FEV1, Forced Expiratory Volume in one second; FVC, Forced Vital Capacity; OCS, Oral corticosteroids; ICS, Inhaled corticosteroids; QIIME, Quantitative Insights into Microbial Ecology; PCoA, principal coordinate analysis; NMDS, Non-metric multidimensional scaling; LC-MS/MS, Liquid Chromatography tandem Mass Spectrometry; UHPLC, Ultra-High-Performance Liquid Chromatography; PCA, Principal component analysis; OPLS-DA, Orthogonal partial least squares-discriminant analysis; VIP, Variable importance in projection; Log₂FC, Log₂FoldChange; PICRUST, Phylogenetic Investigation of Communities by Reconstruction of Unobserved States; ROC, Receiver operating characteristic; AUC, the area under the curve; HC, healthy controls;

WBC, White blood cell; NEU, Neutrophil; LYM, Lymphocyte; MONO, Monocyte; EOS, Eosinophils; BASO, Basophil; 95% CI, 95% Confidence interval; OUT, Operational Taxonomic Units; KEGG, Kyoto Encyclopedia of Genes and Genomes; FDR, False Discovery Rate; IQR, Interquartile range; AA, arachidonic acid.

Data Sharing Statement

The data that support the findings of this study are available on request from the corresponding authors, upon reasonable request.

Ethics Approval and Consent to Participate

Ethical approval for the inclusion of human subjects was granted by the Ethics Committee of The First Affiliated Hospital of Guangzhou Medical University, with approval codes 2022 No.121 and 2024 No. G-007. Written informed consent was secured from all study participants prior to their inclusion in the research.

Acknowledgments

We thank the Immunology Department of the First Affiliated Hospital of Guangzhou Medical University for providing the experimental environment.

Author Contributions

All authors made a significant contribution to the work reported, whether that is in the conception, study design, execution, acquisition of data, analysis and interpretation, or in all these areas; took part in drafting, revising or critically reviewing the article; gave final approval of the version to be published; have agreed on the journal to which the article has been submitted; and agree to be accountable for all aspects of the work.

Funding

The Chinese National Natural Science Foundation (81960023), National Key Research and Development Program of China (2023YFF1203800), Natural Science Foundation of Guangdong Province (2023A1515012917), Natural Science Foundation of Guangdong Province (2024A1515012830), State Key Laboratory Project (SKLRD-Z-202305), Major clinical research project of Guangzhou Medical University (GMUCR2024-02009)(GMUCR2025-02014) Guangdong Provincial Clinical Research Center for Laboratory Medicine (2023B110008),

Disclosure

The authors have declared that no competing interest exists.

References

1. Kiley J, Smith R, Noel P. Asthma phenotypes. *Curr Opin Pulm Med*. 2007;13(1):19–23. doi:10.1097/MCP.0b013e328011b84b
2. Kim HY, Umetsu DT, Dekruyff RH. Innate lymphoid cells in asthma: will they take your breath away? *Eur J Immunol*. 2016;46(4):795–806. doi:10.1002/eji.201444557
3. Pavord ID, Brightling CE, Woltmann G, et al. Non-eosinophilic corticosteroid unresponsive asthma. *Lancet*. 1999;353(9171):2213–2214. doi:10.1016/S0140-6736(99)01813-9
4. Simpson JL, Scott R, Boyle MJ, et al. Inflammatory subtypes in asthma: assessment and identification using induced sputum. *Respirology*. 2006;11(1):54–61. doi:10.1111/j.1440-1843.2006.00784.x
5. Bourdin A, Brusselle G, Couillard S, et al. Phenotyping of severe asthma in the era of broad-acting anti-asthma biologics. *J Allergy Clin Immunol Pract*. 2024;12(4):809–823. doi:10.1016/j.jaip.2024.01.023
6. Sharma S, Gerber AN, Kraft M, et al. Asthma pathogenesis: phenotypes, therapies, and gaps: summary of the aspen lung conference 2023. *Am J Respir Cell Mol Biol*. 2024;71(2):154–168. doi:10.1165/rcmb.2024-0082WS
7. Miller RL, Grayson MH, Strothman K. Advances in asthma: new understandings of asthma's natural history, risk factors, underlying mechanisms, and clinical management. *J Allergy Clin Immunol*. 2021;148(6):1430–1441. doi:10.1016/j.jaci.2021.10.001
8. Stein MM, Hrusch CL, Gozdz J, et al. Innate immunity and asthma risk in Amish and Hutterite Farm Children. *N Engl J Med*. 2016;375(5):411–421. doi:10.1056/NEJMoa1508749
9. Budden KF, Shukla SD, Rehman SF, et al. Functional effects of the microbiota in chronic respiratory disease. *Lancet Respir Med*. 2019;7(10):907–920. doi:10.1016/S2213-2600(18)30510-1

10. Man WH, de Steenhuijsen Piters WA, Bogaert D. The microbiota of the respiratory tract: gatekeeper to respiratory health. *Nat Rev Microbiol.* **2017**;15(5):259–270. doi:10.1038/nrmicro.2017.14
11. Liu B, Li Y, Suo L, et al. Characterizing microbiota and metabolomics analysis to identify candidate biomarkers in lung cancer. *Front Oncol.* **2022**;12:1058436. doi:10.3389/fonc.2022.1058436
12. Taylor SL, Leong LEX, Choo JM, et al. Inflammatory phenotypes in patients with severe asthma are associated with distinct airway microbiology. *J Allergy Clin Immunol.* **2018**;141(1):94–103.e15. doi:10.1016/j.jaci.2017.03.044
13. Li N, Qiu R, Yang Z, et al. Sputum microbiota in severe asthma patients: relationship to eosinophilic inflammation. *Respir Med.* **2017**;131:192–198. doi:10.1016/j.rmed.2017.08.016
14. Perez-Garcia J, González-Carracedo M, Espuela-Ortiz A, et al. The upper-airway microbiome as a biomarker of asthma exacerbations despite inhaled corticosteroid treatment. *J Allergy Clin Immunol.* **2023**;151(3):706–715. doi:10.1016/j.jaci.2022.09.041
15. Ronan V, Yeasin R, Claud EC. Childhood development and the microbiome—the intestinal microbiota in maintenance of health and development of disease during childhood development. *Gastroenterology.* **2021**;160(2):495–506. doi:10.1053/j.gastro.2020.08.065
16. Rinschen MM, Ivanisevic J, Giera M, et al. Identification of bioactive metabolites using activity metabolomics. *Nat Rev Mol Cell Biol.* **2019**;20(6):353–367. doi:10.1038/s41580-019-0108-4
17. Yuan Y, Wang C, Wang G, et al. Airway microbiome and serum metabolomics analysis identify differential candidate biomarkers in allergic rhinitis. *Front Immunol.* **2021**;12:771136. doi:10.3389/fimmu.2021.771136
18. Pang Z, Wang G, Wang C, et al. Serum metabolomics analysis of asthma in different inflammatory phenotypes: a cross-sectional study in Northeast China. *Biomed Res Int.* **2018**;2018:2860521. doi:10.1155/2018/2860521
19. Bateman ED, Hurd SS, Barnes PJ, et al. Global strategy for asthma management and prevention: GINA executive summary. *Eur Respir J.* **2008**;31(1):143–178. doi:10.1183/09031936.00138707
20. Dubin S, Patak P, Jung D. Update on asthma management guidelines. *Mo Med.* **2024**;121(5):364–367. doi:10.1378/chest.130.1_suppl.4s
21. American Thoracic Society. Standards for the diagnosis and care of patients with chronic obstructive pulmonary disease (COPD) and asthma. This official statement of the American Thoracic Society was adopted by the ATS Board of Directors, November 1986. *Am Rev Respir Dis.* **1987**;136(1):225–244. doi:10.1164/ajrccm/136.1.225
22. Schultz A, Balagurusamy S, Dentice R, et al. Thoracic Society of Australia and New Zealand position statement: the safe clinical use of sputum induction for bio-sampling of the lower airways in children and adults. *Respirology.* **2024**;29(5):372–378. doi:10.1111/resp.14707
23. Abi Melhem R, Assaad M, El Gharib K, et al. The determinants of Eosinophilia in patients with severe asthma. *J Clin Med Res.* **2024**;16(4):133–137. doi:10.14740/jocmr5162
24. Lu J, Yao T, Fu S, et al. Metabolomic and microbiomic resilience of Hong Kong oysters to dual stressors: zinc oxide nanoparticles and low salinity. *Chemosphere.* **2024**;368:143722. doi:10.1016/j.chemosphere.2024.143722
25. Magoč T, Salzberg SL. FLASH: fast length adjustment of short reads to improve genome assemblies. *Bioinformatics.* **2011**;27(21):2957–2963. doi:10.1093/bioinformatics/btr507
26. Wang Y, Yu X, Liu F, et al. Respiratory microbiota imbalance in children with *Mycoplasma pneumoniae* pneumonia. *Emerg Microbes Infect.* **2023**;12(1):2202272. doi:10.1080/22221751.2023.2202272
27. Langille MG, Zaneveld J, Caporaso JG, et al. Predictive functional profiling of microbial communities using 16S rRNA marker gene sequences. *Nat Biotechnol.* **2013**;31(9):814–821. doi:10.1038/nbt.2676
28. Sreekumar A, Poisson LM, Rajendiran TM, et al. Metabolomic profiles delineate potential role for sarcosine in prostate cancer progression. *Nature.* **2009**;457(7231):910–914. doi:10.1038/nature07762
29. Haspel JA, Chettimada S, Shaik RS, et al. Circadian rhythm reprogramming during lung inflammation. *Nat Commun.* **2014**;5:4753. doi:10.1038/ncomms5753
30. Heischmann S, Quinn K, Cruickshank-Quinn C, et al. Exploratory metabolomics profiling in the kainic acid rat model reveals depletion of 25-hydroxyvitamin D3 during Epileptogenesis. *Sci Rep.* **2016**;6:31424. doi:10.1038/srep31424
31. Pang Z, Wang G, Gibson P, et al. Airway microbiome in different inflammatory phenotypes of asthma: a cross-sectional study in Northeast China. *Int J Med Sci.* **2019**;16(3):477–485. doi:10.7150/ijms.29433
32. Sverrild A, Kiilerich P, Brejnrod A, et al. Eosinophilic airway inflammation in asthmatic patients is associated with an altered airway microbiome. *J Allergy Clin Immunol.* **2017**;140(2):407–417.e11. doi:10.1016/j.jaci.2016.10.046
33. Greathouse KL, White JR, Vargas AJ, et al. Interaction between the microbiome and TP53 in human lung cancer. *Genome Biol.* **2018**;19(1):123. doi:10.1186/s13059-018-1501-6
34. Yoon HY, Moon SJ, Song JW. Lung tissue microbiome is associated with clinical outcomes of idiopathic pulmonary fibrosis. *Front Med.* **2021**;8:744523. doi:10.3389/fmed.2021.744523
35. Liu H, Zhen C, Xie J, et al. TFAM is an autophagy receptor that limits inflammation by binding to cytoplasmic mitochondrial DNA. *Nat Cell Biol.* **2024**;26(6):878–891. doi:10.1038/s41556-024-01419-6
36. Hu C, Ma Z, Zhu J, et al. Physiological and pathophysiological roles of acidic mammalian chitinase (CHIA) in multiple organs. *Biomed Pharmacother.* **2021**;138:111465. doi:10.1016/j.biopha.2021.111465
37. Kim Y, Li H, Choi J, et al. Glycosidase-targeting small molecules for biological and therapeutic applications. *Chem Soc Rev.* **2023**;52(20):7036–7070. doi:10.1039/D3CS00032J
38. Oh SH, Park S-M, Park J-S, et al. Association analysis of peroxisome proliferator-activated receptors gamma gene polymorphisms with aspirin hypersensitivity in asthmatics. *Allergy Asthma Immunol Res.* **2009**;1(1):30–35. doi:10.4168/air.2009.1.1.30
39. Brasier AR. Interactions between epithelial mesenchymal plasticity, barrier dysfunction and innate immune pathways shape the genesis of allergic airway disease. *Expert Rev Respir Med.* **2025**;19(1):29–41. doi:10.1080/17476348.2024.2449079
40. Hou W, Yu B, Li Y, et al. PC (16:0/14:0) ameliorates hyperoxia-induced bronchopulmonary dysplasia by upregulating claudin-1 and promoting alveolar type II cell repair. *Int J Biochem Cell Biol.* **2024**;172:106587. doi:10.1016/j.biocel.2024.106587
41. Sahu U, Villa E, Reczek CR, et al. Pyrimidines maintain mitochondrial pyruvate oxidation to support de novo lipogenesis. *Science.* **2024**;383(6690):1484–1492. doi:10.1126/science.adh2771
42. Fiore A, Murray PJ. Tryptophan and indole metabolism in immune regulation. *Curr Opin Immunol.* **2021**;70:7–14. doi:10.1016/j.coi.2020.12.001

43. Davidson M, Rashidi N, Nurgali K, et al. The role of tryptophan metabolites in neuropsychiatric disorders. *Int J Mol Sci.* **2022**;23(17):9968. doi:10.3390/ijms23179968
44. Wang B, Wu L, Chen J, et al. Metabolism pathways of arachidonic acids: mechanisms and potential therapeutic targets. *Signal Transduct Target Ther.* **2021**;6(1):94. doi:10.1038/s41392-020-00443-w
45. Kan LL, Li P, Hon SS-M, et al. Deciphering the interplay between the epithelial barrier, immune cells, and metabolic mediators in allergic disease. *Int J Mol Sci.* **2024**;25(13):6913. doi:10.3390/ijms25136913
46. Austen KF. The role of arachidonic acid metabolites in local and systemic inflammatory processes. *Drugs.* **1987**;33(Suppl 1):10–17. doi:10.2165/00003495-198700331-00004

Journal of Asthma and Allergy

Publish your work in this journal

The Journal of Asthma and Allergy is an international, peer-reviewed open-access journal publishing original research, reports, editorials and commentaries on the following topics: Asthma; Pulmonary physiology; Asthma related clinical health; Clinical immunology and the immunological basis of disease; Pharmacological interventions and new therapies. The manuscript management system is completely online and includes a very quick and fair peer-review system, which is all easy to use. Visit <http://www.dovepress.com/testimonials.php> to read real quotes from published authors.

Submit your manuscript here: <https://www.dovepress.com/journal-of-asthma-and-allergy-journal>

Dovepress
Taylor & Francis Group